

A Modelling Assessment of the Impact of Control Measures on Simulated Foot-and-Mouth Disease Spread in Mato Grosso do Sul, Brazil

Nicolas C. Cardenas^a, Jacqueline Marques de Oliveira^b, Andre de Medeiros C. Lins^b, Fernando Endrigo Ramos Garcia^b, Marcus Vinicius Angelo^b, Robson Campos dos Anjos^b, Fabricio de Lima Weber^b, Frederico Bittencourt Fernandes Maia^b, Vanessa Felipe de Souza^c, Gustavo Machado^{*a}

^a*Department of Population Health and Pathobiology, North Carolina State University, Raleigh, NC, USA*

^b*IAGRO, Agência Estadual de Defesa Sanitária Animal e Vegetal, Campo Grande, MS, Brazil*

^c*Embrapa Gado de Corte, Campo Grande, MS, Brazil*

Abstract

This study simulated the introduction of Foot-and-mouth disease (FMD) into Mato Grosso do Sul, Brazil, to evaluate the effectiveness of outbreak control strategies. Our susceptible-exposed-infected-recovered model generated a range of outbreak sizes across the state. These outbreaks were used to model control actions across six scenarios: high vaccination, two variations of moderate depopulation combined with vaccination, high depopulation with limited vaccination, and moderate and high depopulation alone. Our results showed that relying solely on high vaccination was the least effective approach; it controlled only 2.22% of outbreaks and resulted in the highest number of infected farms and the longest control duration. Mixed strategies, busing, moderate depopulation, and vaccination controlled approximately 91% of outbreaks. The use of moderate depopulation alone controlled 96.60% of outbreaks, and it was 14-15 days faster than the mixed approaches. The most effective strategy combined the highest depopulation capacity with limited vaccination, controlling 100% of outbreaks and producing the shortest control duration. The number of vaccinated animals ranged from 211,002 under the optimal strategy to 596,530 when the control strategy included only vaccination. We demonstrated that vaccination alone was insufficient to eliminate outbreaks, and that depopulation and vaccination strategies would be required to stamp out future FMD introduction in Mato Grosso do Sul (MS). The success of such strategy would eliminate between 90% to 100% of outbreaks in 10 to 15 days and reduce the number of infected farms by 10 to 13.

Keywords: Dynamical models, infectious disease control, epidemiology, transmission, targeted control.

Email address: gmachad@ncsu.edu (Gustavo Machado*)

Introduction

Foot-and-mouth disease (FMD) is a highly contagious viral disease affecting cloven-hoofed animals (Brown et al., 2022). It is caused by the FMD virus (FMDV; genus *Aphthovirus*, family *Picornaviridae*). The disease poses a persistent threat to livestock production systems worldwide, with significant implications for both commercial and smallholder farming (Knight-Jones and Rushton, 2013). Following their introduction in the 1960s, vaccines became a cornerstone of FMD control strategies (Sutmoller et al., 2003). In the early 1990s, for instance, mass cattle vaccination campaigns helped eradicate FMD across most of Europe. Upon gaining control, European nations adopted a non-vaccination policy to meet international trade requirements (Sutmoller et al., 2003). Similarly, South American countries, including Argentina, Brazil, Chile, Paraguay, and Uruguay, attained FMD-free status through intensive mass vaccination (Bergmann et al., 2005; Naranjo and Cosivi, 2013).

In the Americas, intensive control and eradication efforts have led to most countries being recognized as FMD-free by the Pan American Health Organization (PAHO, 2020). Despite this progress, the risk of FMD reintroduction remains a major concern, particularly for countries transitioning away from vaccination. In Brazil, the planned cessation of vaccination is expected to increase vulnerability to potential virus incursions. Without the protective buffer conferred by vaccination, the introduction of FMD could spread rapidly through the livestock population, resulting in severe economic losses and trade disruptions (PANAFTOSA et al., 2021; Salvarani et al., 2025). Hence, maintaining robust preparedness and response capacities is essential. Establishing a rapid-response system that incorporates quarantine enforcement, prompt culling of infected animals, and immediate containment measures will be critical to limiting disease spread and mitigating potential impacts (Salvarani et al., 2025).

The economic consequences of FMD outbreaks are well-documented and can be devastating. In Australia, estimated costs range from AUD \$60 million to \$373 million per outbreak. Similarly, during the 2001 outbreaks in the United Kingdom and the Netherlands, more than six million animals were culled, resulting in direct losses of approximately €3.2 billion, with additional impacts on industries such as tourism estimated at between €2.7 and €3.2 billion. In South America, Argentina reported over 2,100 outbreaks, while Uruguay experienced losses of approximately \$730 million and a 1.9% reduction in gross domestic product from 2001 to 2003 (Iriarte et al., 2023; PANAFTOSA et al., 2021; Perez et al., 2004). In Brazil, previous assessments estimated potential economic losses between \$132 million and \$271 million, depending on the severity of trade restrictions (De Menezes et al., 2023). More recently, the 2017–2018 FMD outbreaks in Colombia affected 41 farms, underscoring the continued threat of reintroduction in the region (Iriarte et al., 2023; PANAFTOSA et al., 2021; Perez et al., 2004).

In this context, mathematical models have been developed to simulate the spread of FMD within susceptible animal populations, helping to estimate outbreak sizes, identify high-risk regions, evaluate the effectiveness of control measures, and determine the number of vaccines required to respond to outbreaks in FMD-free countries (Cardenas et al., 2025). These mechanistic models also aid in describing potential outbreak dynamics, estimating economic impacts, and supporting science-based decision-making, ultimately enhancing preparedness and resilience in non-endemic settings (Björnham et al. (2020); Cardenas et al. (2025); Cardenas et al.; Kirkeby

et al. (2021); Pesciaroli et al. (2025); Sanson et al. (2017)).

This study focuses on Mato Grosso do Sul (MS), a Brazilian state with a livestock population of 20,917,525 animals, including cattle, pigs, sheep, and goats (Instituto Brasileiro de Geografia e Estatística (IBGE), 2025), which shares extensive borders with Bolivia and Paraguay. In this study, we develop a stochastic, mechanistic model to simulate the spread of FMD within MS and assess the effectiveness of various control strategies across six intervention scenarios. Specifically, we evaluated outbreak duration, the number of culled animals, and the number of vaccinated animals under each strategy.

Methodology

Data

Population Data

We used data from the official veterinary service of Mato Grosso do Sul (MS), provided by the Agência Estadual de Defesa Sanitária Animal e Vegetal, covering the period from November 30, 2022, to November 30, 2023 (IAGRO, 2025). The dataset covers 103,284 registered farms across 79 municipalities, including 62,894 with bovines, 13,002 with swine, and 7,259 with sheep and goats. Notably, 15,776 farms host more than one species. The spatial distribution of the farms is depicted in Figure 1. In addition, the spatial distribution of the farms by species is depicted in Supplementary Material Figure S1, while the distribution quantity of animals by 10 km by host species is presented in Supplementary Material Figure S2.

Events Data

The dataset captures four primary event types related to animal entry and exit at the farm level: farm-to-farm movements, farm-to-slaughterhouse movements, births, and deaths, provided by (Agência Estadual de Defesa Sanitária Animal e Vegetal, 2026). Farm-to-farm movements accounted for 267,158 records, followed by births (74,005), movements to slaughterhouses (50,740), and deaths (46,913). Death events reflect on-farm mortalities due to causes other than slaughter, distinguishing them from movements to slaughterhouses. Birth and death events are self-reported by farm owners and are required for eligibility for compensation in the event of an outbreak (Governo do Estado de Mato Grosso, 2017). The final dataset comprises 428,643 bovine-related events, 7,512 small ruminant events, and 2,661 swine events recorded between November 1, 2022, and November 30, 2023. The weekly distribution of these events is presented in Supplementary Material Figure S3.

SEIR Model Description

Model Description and Formulation

A multi-host, single-pathogen model, known as MHASpread, was developed by (Cespedes Cardenas and Machado, 2024; Cardenas et al., 2025; Cespedes Cardenas et al., 2024) to simulate FMD outbreaks. The model is based on a susceptible-exposed-infected-recovered (SEIR) compartmental framework, in which the population, comprising bovine, swine, and small ruminants, is

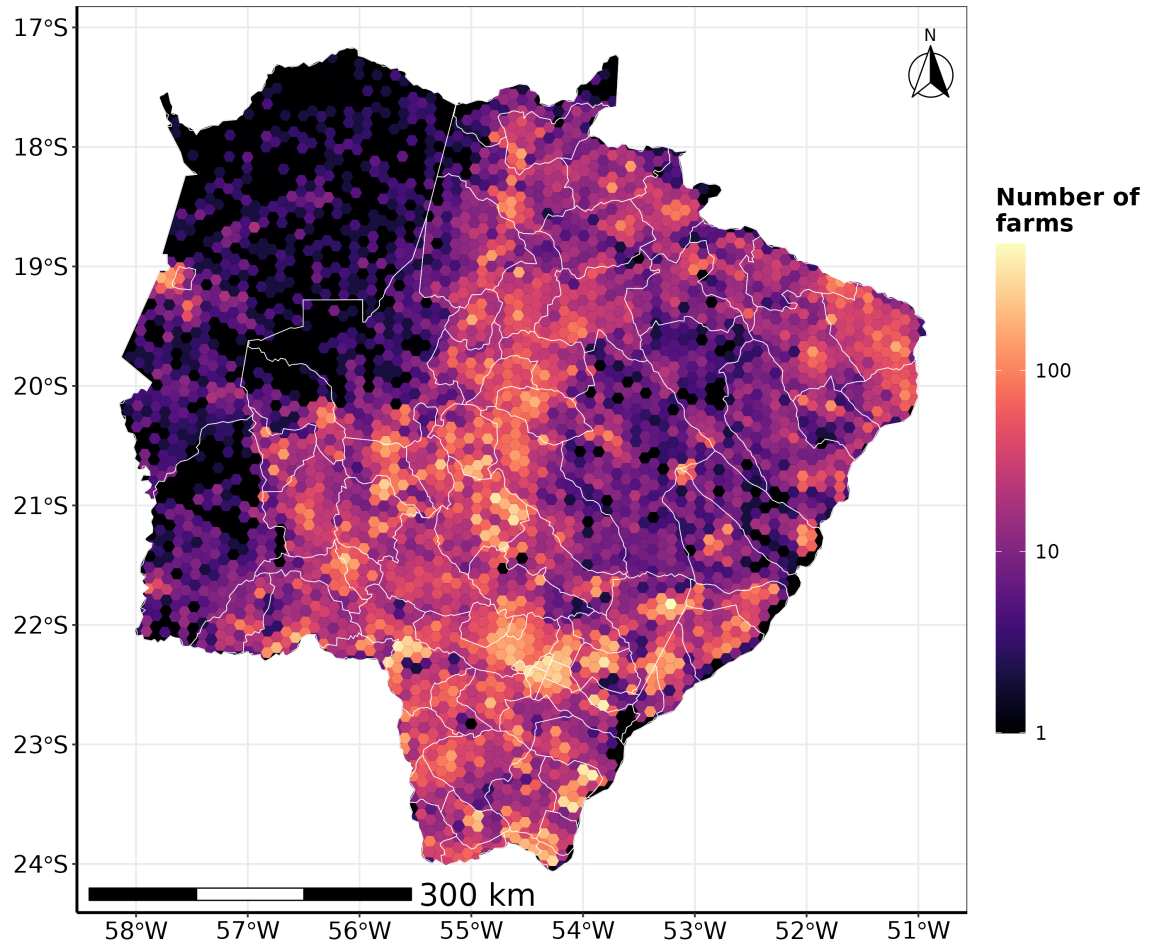


Figure 1: **Farm density represented in a 10 km² hexagon grid.** The hexagon intensity color represents the number of farms allocated; note that the color scale is log₁₀. White lines represent the municipality's division of the state of Mato Grosso do Sul, Brazil.

stratified by species and allocated into four epidemiological compartments. Within each farm, individuals are assumed to mix homogeneously, allowing for direct and indirect transmission among species.

The transmission of FMD within farms is modeled using species-specific transmission probabilities that capture differences in susceptibility and infectiousness across host species. These parameters reflect the heterogeneous transmission dynamics observed in FMD. All within-farm

disease transmission coefficients are summarized in Table 1. Disease progression within each host species follows latent and infectious period distributions presented in Table 2, after which infected animals transition to the recovered compartment and are assumed to be immune for the duration of the simulation.

Between-farm transmission is explicitly modeled through recorded animal movements, with animals transitioning between farms while retaining their epidemiological status. Movements are tracked at the compartment level, accounting for the number of susceptible, exposed, infected, and recovered animals at both origin and destination farms. Movements from farms to slaughterhouses are also included, with transported animals permanently removed from the system and therefore no longer contributing to disease transmission. Similarly, on-farm deaths are modeled as random removals from any compartment. Births are incorporated as new susceptible animals entering the farm population.

In addition to movement-based transmission, spatial transmission between farms is modeled using a distance-dependent transmission kernel, which captures local spread through mechanisms such as airborne transmission, shared equipment, personnel, and wildlife-mediated contacts. The probability of transmission decreases with increasing inter-farm distance, with a maximum effective range of 40 km, consistent with previous FMD modeling studies (Boender and Hagenaars, 2023; Boender et al., 2010). Details of this approach are presented in Supplementary material methods and in (Cespedes Cardenas and Machado, 2024).

Table 1: Host-to-host transmission coefficients (β) per animal⁻¹ day⁻¹.

Species or interaction	Value distribution (min, mode, max)	Reference
Bovine to Bovine	PERT (0.18, 0.24, 0.56)	(da Costa et al., 2022)
Bovine to Swine	PERT (0.18, 0.24, 0.56)	Assumed
Bovine to Small ruminants	PERT (0.18, 0.24, 0.56)	Assumed
Swine to Bovine	PERT (3.7, 6.14, 10.06)	Assumed; (Orsel et al., 2007)
Swine to Swine	PERT (3.7, 6.14, 10.06)	(Eblé et al., 2006)
Swine to Small ruminants	PERT (3.7, 6.14, 10.06)	Assumed; (Orsel et al., 2007)
Small ruminants to Bovine	PERT (0.044, 0.105, 0.253)	Assumed; (Orsel et al., 2007)
Small ruminants to Swine	PERT (0.006, 0.024, 0.09)	(Goris et al., 2009)
Small ruminants to Small ruminants	PERT (0.044, 0.105, 0.253)	(Orsel et al., 2007)

While the progression of the disease through various compartments for each species within the farm population is outlined in Table 2.

Table 2: Within-farm latent and infectious period distributions.

Parameter and species	Mean, median (25th, 75th percentile)	Reference
Latent period (σ), Bovine	3.6, 3 (2, 5)	(Mardones et al., 2010)
Latent period (σ), Swine	3.1, 2 (2, 4)	(Mardones et al., 2010)
Latent period (σ), Small ruminants	4.8, 5 (3, 6)	(Mardones et al., 2010)
Infectious period (γ), Bovine	4.4, 4 (3, 6)	(Mardones et al., 2010)
Infectious period (γ), Swine	5.7, 5 (5, 6)	(Mardones et al., 2010)
Infectious period (γ), Small ruminants	3.3, 3 (2, 4)	(Mardones et al., 2010)

Note: All time units are in days.

A detailed description of the model is provided in the Methods section of the Supplementary Material. The MHASpread framework, which simulates FMD spread within and between farms, is available as R and Python packages and can be looked up at <https://github.com/machado-lab/MHASPREAD-model>.

FMD Spread and Control Actions

Initial conditions

We evaluated six sets of control actions. To ensure comparability, initial outbreak scenarios were generated and then used to simulate countermeasures under different control settings. The outbreaks were simulated by selecting a representative sample of 1,035 farms in Mato Grosso do Sul to serve as initial infected farms, using a multistage, stratified random sampling approach stratified by host species and municipality (Onyeka et al., 2015). Farms were stratified to ensure proportional representation across relevant strata, and the final sample within each stratum was randomly selected. The sample size was determined using Cochran’s formula for finite populations, assuming a 50% prevalence, a 95% confidence level, and a 1.1% margin of error.

The initial infection was introduced by seeding five infected bovines into each selected farm, regardless of population size. If no bovines were present, small ruminants were infected instead, followed by swine if neither species was available. For each selected farm, the model was run for 20 days without control measures, resulting in outbreaks ranging from 1 to 84 farms. These initial outbreaks were used to benchmark the performance of the proposed control scenarios (described below). The spatial distribution of sampled farms is shown in Supplementary Figure S4, while Figure 2 presents the frequency distribution of infected farms.

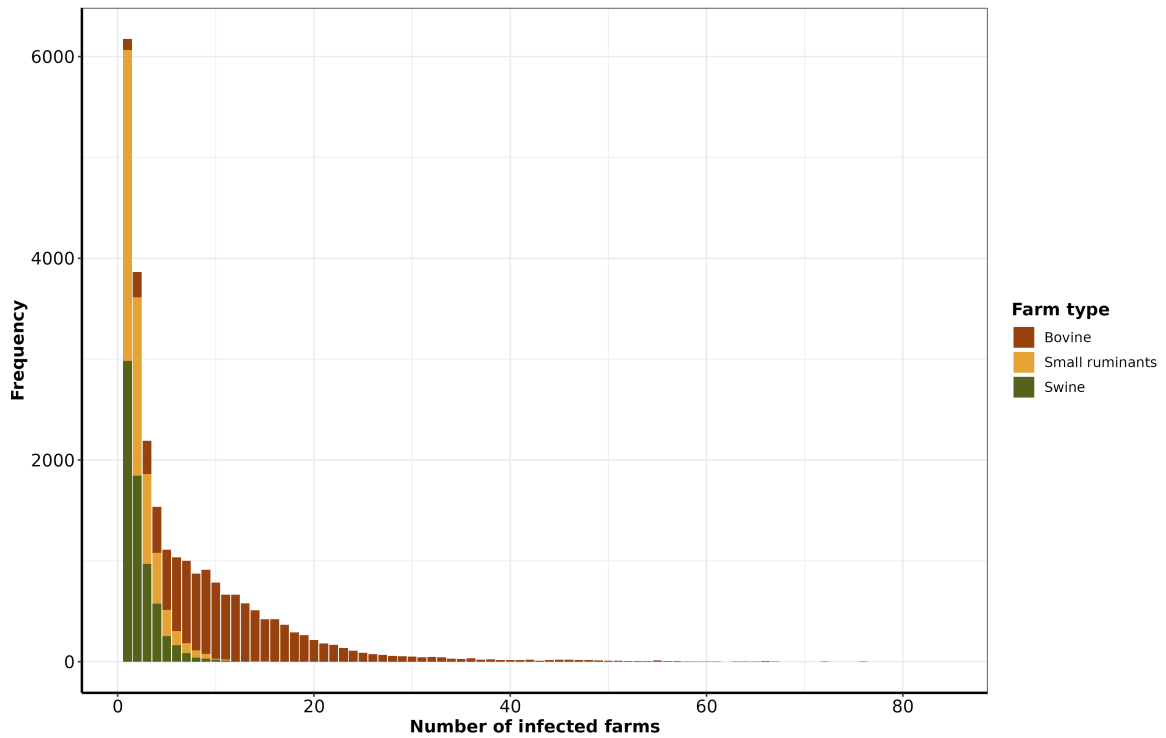


Figure 2: **Initial conditions.** Distribution of secondary infected farms used in the scenarios for the control strategies section of the model. Color represents the presence of at least one species per farm. For mixed-species farms, classification is hierarchical based on the highest-risk species present (bovine > small ruminants > Swine).

Scenarios for control strategies

We outline six distinct control scenarios based on the Brazilian national response plan (MAPA, 2020). These strategies were developed in collaboration with (IAGRO, 2025) animal health officials and were selected to align with local capacities and the organizational structure of the official veterinary service. Each scenario includes establishing three control zones around infected farms and a specific set of countermeasures to contain and eradicate epidemics, including the depopulation rate of infected farms, the emergency vaccination rate, the duration of animal movement standstill, and trace-back settings. The scenario names, rates, and settings of each parameter for each scenario are presented in Table 3.

Table 3 summarizes the parameterization of the epidemiological model across six control scenarios used in the simulation framework, which differ in the intensity and combination of depopulation and vaccination strategies. All scenarios share common initial conditions, with both the initially infected farm and the initial day of simulation selected at random, and a fixed maximum duration of 120 days for the implementation of control actions. Spatial control measures are standardized across scenarios, with infected, buffer, and surveillance zones defined by radii of 3, 5, and 7 km, respectively. Movement restrictions include a 30-day standstill in the surveillance zone in all scenarios, while additional standstills in infected and buffer zones and the depth of

traceback in the contact network vary by scenario, reflecting different levels of tracing intensity. Depopulation strategies range from no depopulation to high capacity daily limits, with some scenarios restricting depopulation exclusively to infected farms and others not applying depopulation at all. Vaccination parameters further differentiate scenarios, including the presence or absence of vaccination, daily vaccination capacity by zone, vaccine efficacy values, species targeted, spatial prioritization of vaccination, and delays to immunity. Collectively, these configurations allow for a systematic comparison of control strategies that vary in operational capacity and intervention mix while maintaining consistent baseline assumptions.

Table 3: Parameters of the model by scenario used in the control action simulations.

Parameter	D0V4	D1V3	D2V2	D2V0	D3V0	D4V1
<i>Initial Conditions</i>						
Infected farm	random	random	random	random	random	random
The initial simulation day	random	random	random	random	random	random
<i>Detection</i>						
Days maximum of control action	120	120	120	120	120	120
<i>Control zone(s) radii in kilometers</i>						
Infected zone	3	3	3	3	3	3
Buffer zone	5	5	5	5	5	5
Surveillance zone	7	7	7	7	7	7
<i>Movement restriction</i>						
Standstill (days)	30	30	30	30	30	30
Standstill in infected zone	F	F	F	F	T	F
Standstill in buffer zone	F	F	F	F	T	F
Standstill in surveillance zone	T	T	T	T	T	T
Traceback steps in the contact network	1	1	1	1	2	1
<i>Depopulation</i>						
Farms depopulated per day (limit)	0	1–2	2–3	2–3	3–4	6–8
Depopulation in infected zone	NA	F	F	F	F	NA
Only depopulate infected farms	NA	T	T	T	T	NA
<i>Vaccination</i>						
Days to achieve immunity	15	15	15	NA	NA	15
Farms vaccinated in buffer zone/day	30–50	25–45	15–30	NA	NA	15–20
Farms vaccinated in infected zone/day	30–50	25–45	15–30	NA	NA	15–20
Vaccine efficacy	0.8, 0.9, 1	0.8, 0.9, 1	0.8, 0.9, 1	NA	NA	0.8, 0.9, 1
Vaccination of swine	F	F	F	NA	NA	F
Vaccination of bovines	T	T	T	NA	NA	T
Vaccination of small ruminants	F	F	F	NA	NA	F
Vaccination in infected zone	T	T	T	NA	NA	T
Vaccination in buffer zone	F	T	T	NA	NA	F
Vaccination delay (days)	15	15	15	NA	NA	15
Vaccination in infectious farms	T	F	T	NA	NA	T

“T” denotes True, indicating that the control action parameter is applied, and “F” is false when control actions were not applied. “NA” signifies Not Applicable, meaning the parameter configuration is not relevant to the current scenario.

We further categorized control scenarios as either “controlled” or “not controlled”. A model simulation was considered “controlled” if no infected farms were present by the end of the simulation. Conversely, a simulation was classified as “not controlled” if the number of infected farms exceeded 400 at any point during the simulation or if control measures extended beyond 100 days while more than one infected farm remained.

Performance of control strategies

To evaluate the performance and differences among the scenarios, we analyzed the percentage of outbreaks successfully controlled under each scenario, the distribution of infected farms at the end of each simulation, the duration of control actions for both controlled and uncontrolled outbreaks, the total number of vaccinated animals, and the total number of depopulated animals at the end of each simulation. The distributions of vaccinated and depopulated animals were further described and compared by assessing frequencies and applying the Kruskal-Wallis rank-sum test to identify significant differences among scenarios. Where significant differences were detected, Dunn’s test with Bonferroni corrections was used for multiple pairwise comparisons.

Number of vaccinated animals

We quantified the total number of vaccinated animals in each simulation and summarized these results using the median and interquartile range. For each simulation, the daily number of vaccinated farms was generated by sampling from a predefined, date-specific vaccination rate specified for each scenario (see 3). Although MHASpread supports vaccination of multiple species, in this study, we restricted vaccination to bovines and buffaloes. We assumed that the vaccine used was homologous to the simulated FMD virus strain and conferred six months of protection with a single dose before a booster dose was required (Ulziibat et al., 2023). Furthermore, we assumed that it required 15 days to achieve immunization coverage levels of 0.8, 0.9, or 1.0; at each simulation run, the model randomly sampled one of these coverage levels. Under these assumptions, we calculated the number of animals to be vaccinated rather than the number of vaccine doses administered. Vaccination of cattle was implemented in both infected and buffer zones (Table 3).

Furthermore, in our model, depopulation is prioritized over vaccination, while depopulated farms are excluded from immunization because no animals remain to be vaccinated. Conversely, if animals are vaccinated and subsequently depopulated, they are still recorded as vaccinated even if depopulation occurs in the following days. The control zone area (infected and/or buffer) and the number of farms vaccinated per day were determined according to each scenario (Table 3).

Software

The MHASpread model was initially developed in Python v. 3.8.12 and subsequently analyzed in R v. 4.2.3 (R Core Team, 2025) to create graphics, tables, and maps. In Python, the analysis relied on the following packages: NumPy (Harris et al., 2020), Pandas (McKinney, 2010), and SciPy (Virtanen et al., 2020). In R, the following packages were used: sampler (Baldassaro, 2019), tidyverse (Wickham et al., 2019), sf (Pebesma, 2018), doParallel (Corporation and Weston, 2022), and lubridate (Grolemund and Wickham, 2011).

Results

General results

We assessed the median number of infected farms at the end of each simulation. The overall median number of infected farms was 51 (interquartile range: 33–79; maximum: 309). Significant differences were observed among scenarios when comparing the distribution of the total number of infected farms at the end of the simulations (Table 4). Scenario D1V3 differed significantly from D0V4 and D2V2 ($p = 0.0032$ and $p = 0.0013$, respectively), demonstrating the benefits of the vaccination strategy combined with moderate depopulation in terms of outbreak containment compared with scenarios with either higher vaccination (D0V4) or different depopulation levels (D2V2). Scenario D3V0 showed significant differences compared to D1V3, D2V0, and D2V2 ($p < 0.0001$), reflecting the impact of intensive depopulation without vaccination, which reduced both the outbreak duration and the total number of infected farms. Scenario D4V1 was distinct from all other scenarios ($p < 0.0001$), achieving full outbreak control through a highly targeted combination of rapid depopulation and limited vaccination, resulting in fewer infected farms, shorter control durations, and lower total vaccination requirements. These differences are presented in Supplementary Material Figure S5.

Table 4: Performance metrics for disease control simulation scenarios, organized by the percentage of controlled outbreaks. The parameters include the percentage of outbreaks controlled, the duration in days of control actions, the number of vaccinated animals, the number of depopulated animals, and the total infected farms, with each parameter showing median, interquartile range, and maximum values.

Scenario	Controlled Outbreaks (%)	Total Infected Farms (med, IQR, max)	Days on Control (med, IQR, max)	Vaccinated Animals (med, IQR, max)	Depopulated Animals (med, IQR, max)
D0V4	2.22	17 (9.5–37.5, 80)	26 (23–52, 71)	596,530 (350,817–938,389, 3,844,170)	0 —
D2V2	90.52	54 (36–76, 187)	36 (22–53, 95)	447,278 (258,465–680,058, 2,711,163)	30,894 (18,383–46,762, 317,969)
D1V3	90.96	54 (36–77, 195)	35 (22–53, 96)	434,240 (256,107–679,540, 2,685,043)	30,444 (18,107–48,384, 368,609)
D2V0	96.60	53 (33–85, 273)	21 (12–35, 96)	0 —	33,097 (19,387–53,072, 566,938)
D3V0	99.90	48 (30–75, 286)	14 (8–22, 95)	0 —	31,467 (18,393–50,620, 504,437)
D4V1	100	41 (27–61, 206)	6 (4–9, 41)	211,002 (94,520–378,256, 1,127,699)	28,976 (16,836–45,627, 433,797)

Number of vaccinated animals by scenario

The distribution of vaccinated animals at the end of each simulation by scenario is presented in Figure 3. The number of vaccinated animals differs significantly across scenarios. Scenario D0V4 showed the highest median number of vaccinated animals at 596,530, which was significantly higher compared to D1V3 and D2V2 ($p = 0.0032$ and $p = 0.0013$, respectively). Scenario D2V2 was the second with the most vaccine use, with a median of 447,278 vaccinated bovines, reflecting a moderate reduction from D0V4, and no significant difference compared to D1V3 ($p > 0.5$). Similarly, scenario D1V3 has a median of 434,240 vaccinated animals. In contrast, scenario D4V1 exhibits the lowest vaccination numbers among all scenarios, with a median of 211,002, showing significant differences from all other scenarios ($p < 0.0001$). The results of all pair comparisons are presented in the Supplementary Material Figure S6.

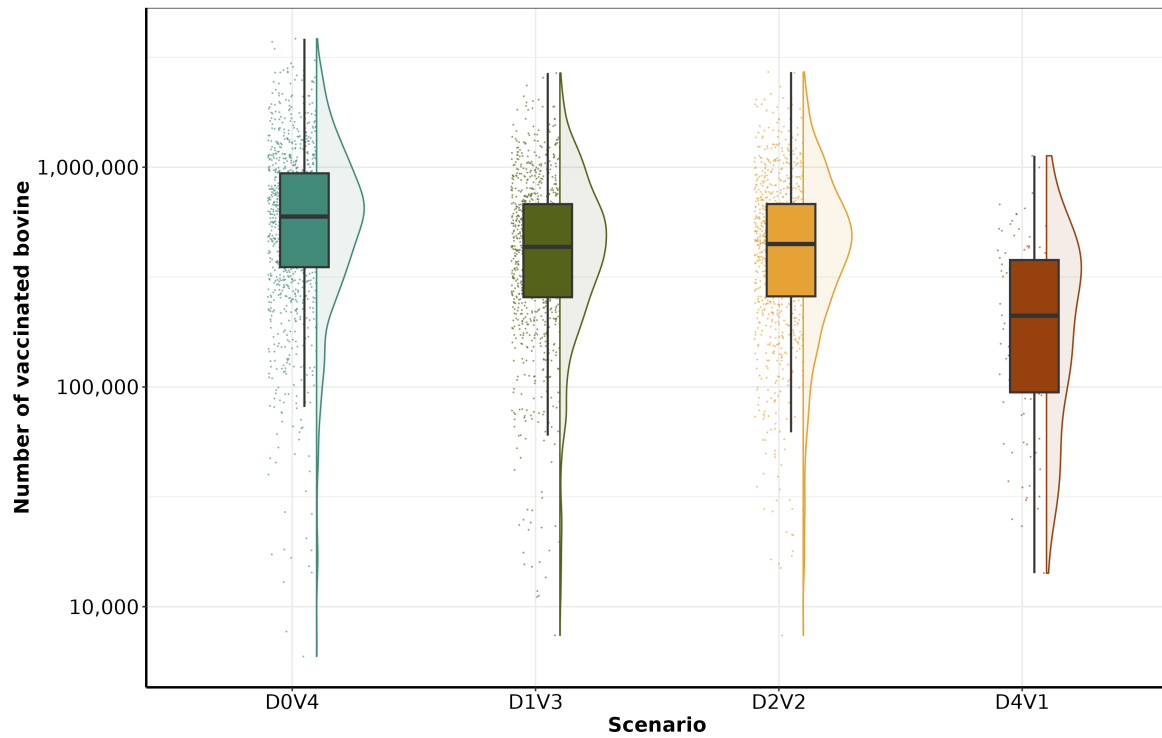


Figure 3: **Distribution of the total vaccinated bovines. The y-axis denotes the number of vaccinated bovines, while the x-axis represents simulated scenarios.** The dots and shaded area represent the distribution of individual simulations.

Number of depopulated animals

The distribution of depopulated animals at the end of each simulation is depicted in Figure 4, and the complete results are shown in Table 4. Overall, the number of depopulated animals varied widely across simulations, with a median from 28,976 to 33,097 and ranging from 1,042 to 566,938. The highest number of depopulated animals were D2V0, D3V0, and D2V2, with medians of 33,097 (max: 566,938), 31,467 (max: 504,437), and 30,894 (max: 317,969), respectively. Significant differences were observed between D4V1 to D2V0 ($p < 0.0001$), D4V1 to D2V2 ($p = 0.012$), and D4V1 to D1V3 ($p = 0.032$), as well as between D4V1 and D3V0 ($p = 0.044$). The results of all pairwise comparisons are provided in Supplementary Material Figure S6.

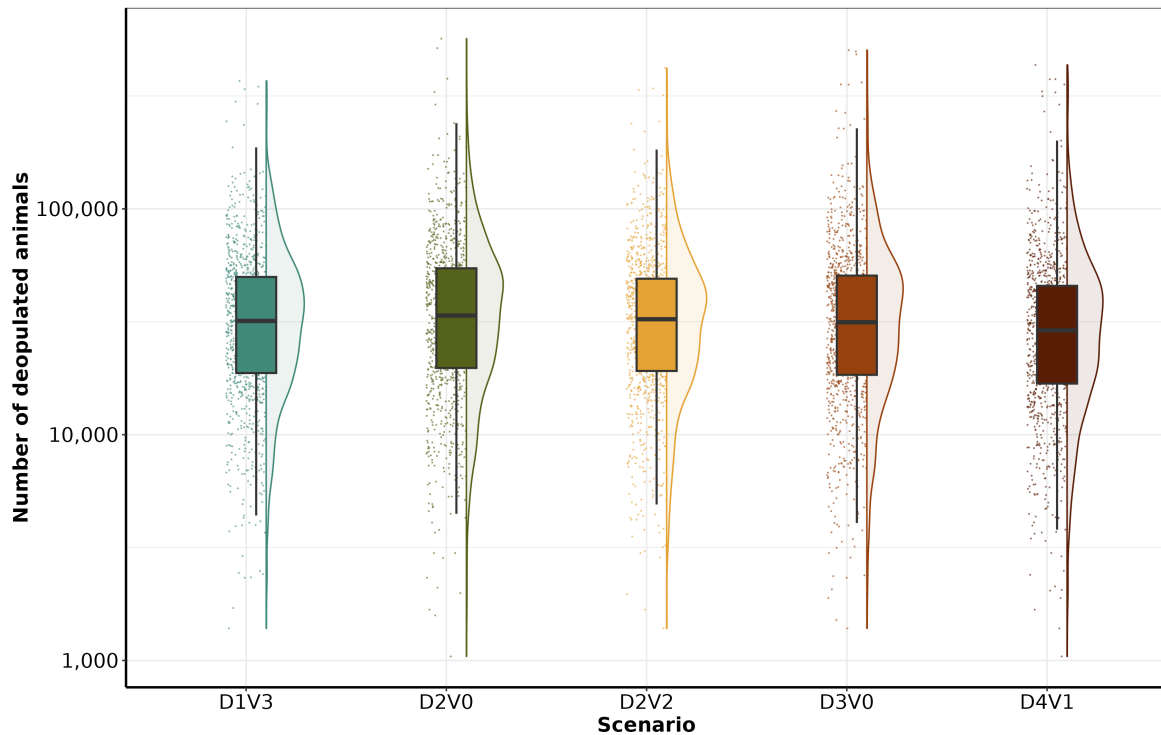


Figure 4: **Distribution of number of depopulated animals.** The y-axis denotes the number of depopulated animals, while the x-axis represents simulated scenarios. The dots and shaded area represent the distribution of individual simulations.

Discussion

This study applied the MHASpread model to simulate the potential dissemination of FMD in Mato Grosso do Sul, Brazil, and to assess the effectiveness of the broad array of control strategies included in the Brazilian national response plan (MAPA, 2020). We assessed six control scenarios designed to contain and mitigate disease spread under different combinations of depopulation and vaccination. Integrated control strategies combining depopulation and vaccination were consistently the most effective, as they simultaneously reduced the number of infectious animals and limited onward transmission through the development of population immunity.

Scenarios that incorporated both depopulation and vaccination (D1V3, D2V2, and D4V1) achieved the highest outbreak control rates, ranging from 90.52% to 100% within a median of 36 (IQR: 22–53) and 6 (IQR: 4–9) days, respectively. This occurs because depopulation rapidly removes infectious and high-risk animals, while vaccination progressively reduces susceptibility among remaining populations (Iriarte et al., 2023; Roche et al., 2015). In contrast, vaccination alone was insufficient to eliminate all outbreaks, as vaccine-induced immunity requires time to develop and does not immediately interrupt transmission during the early phase of an outbreak (Iriarte et al., 2023; Roche et al., 2015).

Scenarios D1V3 and D2V2 required longer control periods, with median durations of 54 days (IQR 36–77) and 36 days (IQR 22–53), respectively, compared with depopulation-only strategies, which achieved control 15 to 40 days faster, while maintaining similarly high outbreak control rates. This is explained by the delay between vaccination and the acquisition of protective immunity, during which residual transmission can continue and prolong control efforts (Porphyre et al., 2013). Consequently, vaccination may initially slow outbreak resolution when not paired with sufficiently rapid and targeted depopulation; such events have been described in the Argentina outbreak in 2001 (Perez et al., 2004).

By contrast, scenario D4V1 demonstrates that when vaccination is optimally integrated with depopulation, the duration of control actions can be substantially reduced. In this scenario, depopulation effectively decreases early transmission, while limited but well-targeted vaccination reduces susceptibility in surrounding at-risk farms, preventing secondary spread. As a result, D4V1 achieved complete outbreak control with a median duration of six days (IQR: 4–9; maximum: 41 days). These findings indicate that vaccination does not inherently shorten control periods when combined with depopulation; rather, its impact depends on the intensity, timing, and spatial targeting of vaccination, as well as its coordination with depopulation strategies aimed at infected and high-risk farms. This result agrees with similar simulation studies in Bolivia, Brazil, Thailand, and Italy (Cardenas et al., 2025; Cespedes Cardenas et al., 2024; Wongnak et al., 2024; Pesciaroli et al., 2025; Bellini et al., 2025).

Vaccination alone was largely ineffective, as shown by D0V4, which achieved only 2.22% outbreak control. Depopulation alone, as in D3V0, achieved high efficacy (99.90%) with 14 days of control (IQR: 8–22), indicating that depopulation is highly effective; however, it may be operationally demanding (Knight-Jones and Rushton, 2013; Wittwer, 2024). Overall, in our simulation in Mato Grosso do Sul, the duration of control actions was closely linked to the number of depopulated and vaccinated animals. Scenarios relying primarily on depopulation, such as D3V0, required longer intervention periods due to logistical challenges of large-scale culling. In contrast, D4V1, which integrated vaccination, significantly reduced control duration while also decreasing the median number of depopulated animals (28,976; IQR: 16,836–45,627) compared to D3V0 (31,467; IQR: 18,393–50,620). Interestingly, high-intensity depopulation reduces the number of vaccinated animals. In D4V1, a median of 211,002 (IQR: 94,520–378,256) animals were vaccinated, which is 51.4% fewer than in D1V3 (434,240 animals vaccinated), while the median number of depopulated animals decreased only slightly (4.8%) compared to D1V3 (30,444 depopulated). Similar results were reported in simulated outbreaks in the central United States and Australia (Capon et al., 2021; McReynolds et al., 2014; Yadav et al., 2022). This is because an effective depopulation from the outset helps prevent secondary infections, reducing the need for additional control zones and ultimately leading to fewer vaccinated animals (Backer et al., 2012; Capon et al., 2021; Cardenas et al., 2025). Despite the strong performance of depopulation alone, our results suggest that early detection combined with small outbreak size allows depopulation to effectively eliminate outbreaks without additional intervention. However, in cases of large-scale outbreaks, vaccination creates a synergy with depopulation that enables more efficient mitigation and control, as demonstrated in large outbreaks in Argentina and Uruguay (Iriarte et al., 2023; Perez et al., 2004). The MHASpread model was also applied in Bolivia (Cardenas et al., 2025), Rio Grande do Sul (RS) (Cespedes Cardenas et al., 2024), Brazil, which allows for contrasting

some vaccine numbers under comparable modeling settings. In Bolivia, a median of 1,962 animals were vaccinated per day (IQR: 726 to 6,752), with 50 to 90 farms vaccinated per day. RS achieved a similar median of 1,928 animals per day (IQR: 1,562 to 3,567; maximum: 20,740), but with higher per-farm capacity, vaccinating approximately 20 farms per day. In contrast, MS operated at a substantially larger scale, with a median of 9,247 animals vaccinated per day (IQR: 4,702 to 16,770), vaccinating 60 to 100 farms per day. Under these settings, Bolivia controlled approximately 60% of cases, whereas RS and MS achieved outbreak control rates exceeding 90%. Across all scenarios, the depopulation rate remained consistent at 1 to 2 farms per day, highlighting that vaccination requirements are strongly influenced by population density and vaccination intensity. Consequently, the number of animals requiring vaccination cannot be reliably determined by direct extrapolation from other regions (Cardenas et al., 2025; Cespedes Cardenas et al., 2024; Meadows et al., 2018).

Limitations and further remarks

While the MHASpread model (Cespedes Cardenas and Machado, 2024) provides insights into the dynamics of FMD transmission, but limitations should be acknowledged. First, the model assumes homogeneous mixing of animals within farms, which may oversimplify intra-farm transmission processes. In reality, contact patterns are often structured by production stage, housing, and management practices (Instituto Brasileiro de Geografia e Estatística, 2017). Future extensions could incorporate heterogeneous contact structures to better represent within-farm transmission dynamics (Cabezas et al., 2020; Craft, 2015).

The model relies on historical animal movement and population data, which may not fully reflect real-time changes. The absence of historical FMD outbreaks in the study region further limited our ability to calibrate and validate the model (Hazelbag et al., 2020). As a result, epidemiological parameters were derived from the literature rather than estimated from observed outbreak data, and independent validation using epidemic trajectories was not performed. The analysis is geographically restricted to a single state. Although the findings are relevant to livestock systems with similar structural characteristics, extrapolation to other regions should be approached with caution, as differences in farm density, production systems, and movement patterns may influence disease dynamics and control effectiveness.

Finally, while no major data gaps were identified, the analysis depends on official registries, and the potential absence of unregistered farms cannot be entirely excluded. Farm population sizes and demographic events are self-reported by producers. In addition, illegal or unreported animal movements could not be incorporated due to data limitations. Nevertheless, this is unlikely to have substantially affected the results, as animal movements require official authorization and are restricted to the number of animals registered in the system. The volume of information is sufficient to provide a representation of the state, as all animal movements require state authorization and are limited to the total number of animals permitted. The authors will continue to develop and refine the MHSpread model, with the objectives of improving computational efficiency, enhancing usability, and extending its applicability to other diseases and analytical tasks, including the economic assessment of outbreaks (Cardenas et al.), finally future works will assess the number of required vaccine doses over different outbreak sizes.

Conclusion

We demonstrated that integrated scenarios combining vaccination and depopulation are significantly more effective than single-method approaches, achieving containment rates between 90.96% and 100%. While vaccination alone was ineffective, controlling only 2.22% of outbreaks, its integration with depopulation substantially improved outcomes. For instance, D4V1 achieved 100% control with a median of 6 days to contain the outbreak, compared with 14 days in the depopulation-only scenario. Moreover, high-intensity depopulation requires fewer animals to be depopulated, as it prevents the onset of new cases. The likelihood of FMD eradication depends on maintaining adequate vaccine coverage, rapid deployment, and the capacity to depopulate on a daily basis. Under our specific control strategies, the median number of animals that were vaccinated ranged from 211,002 to 596,530, whereas the number of animals subjected to depopulation varied from 28,976 to 33,097. Early detection and swift implementation of control measures remain critical for outbreak containment and minimizing epidemic duration.

Acknowledgments

We would like to thank the animal health officials of agência Estadual de Defesa Sanitária Animal e Vegetal, Campo Grande, MS, Brazil (IAGRO) for their constant contributions to discussions regarding the state FMD response plan.

Funding statement

This work was supported by the Machado Laboratory at the Department of Population Health and Pathobiology, College of Veterinary Medicine, North Carolina State University, Raleigh, NC, USA.

Data Availability Statement

The data supporting this study's findings are not publicly available and are protected by confidential agreements; therefore, they are not available.

References

- Agência Estadual de Defesa Sanitária Animal e Vegetal, 2026. Agência estadual de defesa sanitária animal e vegetal (iagro). URL: <https://www.iagro.ms.gov.br/>. official website of the state agency responsible for animal and plant health defense in Mato Grosso do Sul, Brazil. Accessed February 1, 2026.
- Backer, J., Hagenaars, T., Nodelijk, G., van Roermund, H., 2012. Vaccination against foot-and-mouth disease i: Epidemiological consequences. *Preventive Veterinary Medicine* 107, 27–40. URL: <https://linkinghub.elsevier.com/retrieve/pii/S0167587712001687>, doi:10.1016/j.prevetmed.2012.05.012.

- Baldassaro, M., 2019. *sampler: Sample design, drawing & data analysis using data frames*. URL: <https://CRAN.R-project.org/package=sampler>. r package, accessed 2024-09-16.
- Bellini, S., Scaburri, A., Tironi, M., Cappa, V., Mannelli, A., Alborali, G.L., 2025. Simulating the Spread of Foot-and-Mouth Disease in Densely Populated Areas as Part of Contingency Plans to Establish the Best Control Options. *Pathogens* 14, 933. URL: <https://www.mdpi.com/2076-0817/14/9/933>, doi:10.3390/pathogens14090933.
- Bergmann, I.E., Malirat, V., Falczuk, A.J., 2005. Evolving perception on the benefits of vaccination as a foot and mouth disease control policy: contributions of South America. *Expert Review of Vaccines* 4, 903–913. URL: <http://www.tandfonline.com/doi/full/10.1586/14760584.4.6.903>, doi:10.1586/14760584.4.6.903.
- Björnham, O., Sigg, R., Burman, J., 2020. Multilevel model for airborne transmission of foot-and-mouth disease applied to swedish livestock. *PLOS ONE* 15, e0232489. URL: <https://dx.plos.org/10.1371/journal.pone.0232489>, doi:10.1371/journal.pone.0232489.
- Boender, G.J., Hagenaars, T.J., 2023. Common features in spatial livestock disease transmission parameters. *Scientific Reports* 13, 3550. URL: <https://www.nature.com/articles/s41598-023-30230-w>, doi:10.1038/s41598-023-30230-w.
- Boender, G.J., van Roermund, H.J., de Jong, M.C., Hagenaars, T.J., 2010. Transmission risks and control of foot-and-mouth disease in the netherlands: Spatial patterns. *Epidemics* 2, 36–47. URL: <https://linkinghub.elsevier.com/retrieve/pii/S1755436510000174>, doi:10.1016/j.epidem.2010.03.001.
- Brown, E., Nelson, N., Gubbins, S., Colenutt, C., 2022. Airborne transmission of foot-and-mouth disease virus: A review of past and present perspectives. *Viruses* 14, 1009. URL: <https://www.mdpi.com/1999-4915/14/5/1009>, doi:10.3390/v14050901.
- Cabezas, A.H., Sanderson, M.W., Volkova, V.V., 2020. A meta-population model of potential foot-and-mouth disease transmission, clinical manifestation, and detection within u.s. beef feedlots. *Frontiers in Veterinary Science* Volume 7 - 2020. URL: <https://www.frontiersin.org/journals/veterinary-science/articles/10.3389/fvets.2020.527558>, doi:10.3389/fvets.2020.527558.
- Capon, T.R., Garner, M.G., Tapsuwan, S., Roche, S., Breed, A.C., Liu, S., Miller, C., Bradhurst, R., Hamilton, S., 2021. A simulation study of the use of vaccination to control foot-and-mouth disease outbreaks across australia. *Frontiers in Veterinary Science* 8, 648003. URL: <https://www.frontiersin.org/articles/10.3389/fvets.2021.648003/full>, doi:10.3389/fvets.2021.648003.
- Cardenas, N.C., de Menezes, T.C., Countryman, A.M., Lopes, F.P.N., Groff, F.H.S., Rigon, G.M., Gocks, M., Machado, G., . Integrating epidemiological and economic models to estimate the cost of simulated foot-and-mouth disease outbreaks in brazil. URL: <https://arxiv.org/abs/2502.07083>, doi:10.48550/ARXIV.2502.07083. version Number: 1.

- Cardenas, N.C., Santos, D.V.D., Lima, D.M., Gutierrez, H.O.D., Vaca, D.R.G., Machado, G., 2025. Foot-and-mouth disease in bolivia: Simulation-based assessment of control strategies and vaccination requirements. *Transboundary and Emerging Diseases* 2025, 9055612. URL: <https://onlinelibrary.wiley.com/doi/10.1155/tbed/9055612>, doi:10.1155/tbed/9055612.
- Cespedes Cardenas, N., Amadori Machado, F., Trois, C., Maran, V., Machado, A., Machado, G., 2024. Modeling foot-and-mouth disease dissemination in rio grande do sul, brazil and evaluating the effectiveness of control measures. *Frontiers in Veterinary Science* 11. URL: <https://www.frontiersin.org/journals/veterinary-science/articles/10.3389/fvets.2024.1468864>, doi:<https://doi.org/10.3389/fvets.2024.1468864>.
- Cespedes Cardenas, N., Machado, G., 2024. Mhaspread model. URL: <https://github.com/machado-lab/MHASPREAD-model>. gitHub repository, accessed 2024-09-16.
- Corporation, M., Weston, S., 2022. doParallel: Foreach parallel adaptor for the 'parallel' package. URL: <https://CRAN.R-project.org/package=doParallel>.
- da Costa, J.M.N., Cobellini, L.G., Cardenas, N.C., Groff, F.H.S., Machado, G., 2022. Assessing epidemiological parameters and dissemination characteristics of the 2000 and 2001 foot-and-mouth disease outbreaks in rio grande do sul, brazil. *bioRxiv*, 2022.05.22.492961 URL: <http://biorxiv.org/content/early/2022/05/24/2022.05.22.492961.abstract>, doi:10.1101/2022.05.22.492961.
- Craft, M.E., 2015. Infectious disease transmission and contact networks in wildlife and livestock. *Philosophical Transactions of the Royal Society B: Biological Sciences* 370, 20140107. URL: <https://royalsocietypublishing.org/doi/10.1098/rstb.2014.0107>, doi:10.1098/rstb.2014.0107.
- De Menezes, T.C., Ferreira Filho, J.B.D.S., Countryman, A.M., 2023. Potential economic impacts of foot-and-mouth disease in brazil: A case study for mato grosso and paran. *Journal of the Agricultural and Applied Economics Association* 2, 481–496. URL: <https://onlinelibrary.wiley.com/doi/10.1002/jaa2.73>, doi:10.1002/jaa2.73.
- Ebl, P., De Koeijer, A., Bouma, A., Stegeman, A., Dekker, A., 2006. Quantification of within- and between-pen transmission of Foot-and-Mouth disease virus in pigs. *Veterinary Research* 37, 647–654. URL: <http://www.edpsciences.org/10.1051/vetres:2006026>, doi:10.1051/vetres:2006026.
- Goris, N.E., Ebl, P.L., Jong, M.C.M.d., Clercq, K.D., 2009. Quantifying foot-and-mouth disease virus transmission rates using published data. *ALTEX - Alternatives to animal experimentation* 26, 52–54. URL: <https://www.altex.org/index.php/altex/article/view/637>, doi:10.14573/altex.2009.1.52. number: 1.
- Governo do Estado de Mato Grosso, 2017. Decreto 1.260, de 10 de novembro de 2017, que regulamenta a lei estadual n

- deg 10.486, de 29 de dezembro de 2016, que dispõe sobre a defesa sanitária animal no estado de mato grosso e dá outras providências. Legislação estadual de Mato Grosso. URL: <https://iframe.leisestaduais.com.br/mt/decreto-n-1260-2017-mato-grosso-regulamenta-a-lei-estadual-no-10-486-de-29-de-dezembro-publicado-no-Diário-Oficial-do-Estado-de-Mato-Grosso-em-10-de-novembro-de-2017;consolidado-com-alterações-posteriores-até-2025>.
- Grolemund, G., Wickham, H., 2011. Dates and times made easy with {lubridate}. *Journal of Statistical Software* 40, 1–25. URL: <https://www.jstatsoft.org/v40/i03/>. publisher: CRAN.
- Harris, C.R., Millman, K.J., van der Walt, S.J., Gommers, R., Virtanen, P., Cournapeau, D., Wieser, E., Taylor, J., Berg, S., Smith, N.J., Kern, R., Picus, M., Hoyer, S., van Kerkwijk, M.H., Brett, M., Haldane, A., del Río, J.F., Wiebe, M., Peterson, P., Gérard-Marchant, P., Sheppard, K., Reddy, T., Weckesser, W., Abbasi, H., Gohlke, C., Oliphant, T.E., 2020. Array programming with NumPy. *Nature* 585, 357–362. URL: <https://doi.org/10.1038/s41586-020-2649-2>, doi:10.1038/s41586-020-2649-2.
- Hazelbag, C.M., Dushoff, J., Dominic, E.M., Mthombothi, Z.E., Delva, W., 2020. Calibration of individual-based models to epidemiological data: A systematic review. *PLOS Computational Biology* 16, 1–17. URL: <https://doi.org/10.1371/journal.pcbi.1007893>, doi:10.1371/journal.pcbi.1007893.
- IAGRO, ., 2025. IAGRO - agência estadual de defesa sanitária animal e vegetal. URL: <https://www.iagro.ms.gov.br/>.
- Instituto Brasileiro de Geografia e Estatística, 2017. Censo agropecuário 2017. Official webpage with statistics and metadata on the 2017 Agricultural Census. URL: <https://www.ibge.gov.br/estatisticas/economicas/agricultura-e-pecuaria/21814-2017-censo-agropecuario.html>. accessed: 2026-02-10.
- Instituto Brasileiro de Geografia e Estatística (IBGE), 2025. Municipal livestock production. Online. URL: <https://www.ibge.gov.br/en/statistics/full-list-statistics/17353-municipal-livestock-production.html?edicao=31810&t=resultados>. accessed: 2026-02-02.
- Iriarte, M.V., Gonzáles, J.L., De Freitas Costa, E., Gil, A.D., De Jong, M.C.M., 2023. Main factors associated with foot-and-mouth disease virus infection during the 2001 FMD epidemic in uruguay. *Frontiers in Veterinary Science* 10, 1070188. URL: <https://www.frontiersin.org/articles/10.3389/fvets.2023.1070188/full>, doi:10.3389/fvets.2023.1070188.
- Kirkeby, C., Brookes, V.J., Ward, M.P., Dürr, S., Halasa, T., 2021. A practical introduction to mechanistic modeling of disease transmission in veterinary science. *Frontiers in Veterinary Science* 7, 546651. URL: <https://www.frontiersin.org/articles/10.3389/fvets.2020.546651/full>, doi:10.3389/fvets.2020.546651.

- Knight-Jones, T., Rushton, J., 2013. The economic impacts of foot and mouth disease – What are they, how big are they and where do they occur? *Preventive Veterinary Medicine* 112, 161–173. URL: <https://linkinghub.elsevier.com/retrieve/pii/S0167587713002390>, doi:10.1016/j.prevetmed.2013.07.013.
- MAPA, 2020. Febre aftosa. URL: <https://www.gov.br/agricultura/pt-br/assuntos/saude-animal-e-vegetal/saude-animal/programas-de-saude-animal/febre-aftosa/febre-aftosa>.
- Mardones, F., Perez, A., Sanchez, J., Alkhamis, M., Carpenter, T., 2010. Parameterization of the duration of infection stages of serotype o foot-and-mouth disease virus: an analytical review and meta-analysis with application to simulation models. *Veterinary Research* 41, 45. URL: <http://www.vetres.org/10.1051/vetres/2010017>, doi:10.1051/vetres/2010017.
- McKinney, W., 2010. Data structures for statistical computing in python. *Proceedings of the 9th Python in Science Conference* 445, 51–56. doi:10.25080/Majora-92bf1922-00a.
- McReynolds, S.W., Sanderson, M.W., Reeves, A., Hill, A.E., 2014. Modeling the impact of vaccination control strategies on a foot and mouth disease outbreak in the central united states. *Preventive Veterinary Medicine* 117, 487–504. URL: <https://linkinghub.elsevier.com/retrieve/pii/S0167587714003213>, doi:10.1016/j.prevetmed.2014.10.005.
- Meadows, A.J., Mundt, C.C., Keeling, M.J., Tildesley, M.J., 2018. Disentangling the influence of livestock vs. farm density on livestock disease epidemics. *Ecosphere* 9, e02294. URL: <https://esajournals.onlinelibrary.wiley.com/doi/10.1002/ecs2.2294>, doi:10.1002/ecs2.2294.
- Naranjo, J., Cosivi, O., 2013. Elimination of foot-and-mouth disease in South America: lessons and challenges. *Philosophical Transactions of the Royal Society B: Biological Sciences* 368, 20120381. URL: <https://royalsocietypublishing.org/doi/10.1098/rstb.2012.0381>, doi:10.1098/rstb.2012.0381.
- Onyeka, A.C., Izunobi, C.H., Iwueze, I.S., 2015. Estimation of Population Ratio in Post-Stratified Sampling Using Variable Transformation. *Open Journal of Statistics* 05, 1–9. URL: <http://www.scirp.org/journal/doi.aspx?DOI=10.4236/ojs.2015.51001>, doi:10.4236/ojs.2015.51001.
- Orsel, K., Dekker, A., Bouma, A., Stegeman, J., De Jong, M., 2007. Quantification of foot and mouth disease virus excretion and transmission within groups of lambs with and without vaccination. *Vaccine* 25, 2673–2679. URL: <https://linkinghub.elsevier.com/retrieve/pii/S0264410X06012692>, doi:10.1016/j.vaccine.2006.11.048.
- PAHO, 2020. Diagnóstico diferencial de enfermedades vesiculares en bovinos. OPS. URL: https://iris.paho.org/bitstream/handle/10665.2/51259/diagnosticodiferencial_spa.pdf?sequence=1&isAllowed=y.

- PANAFTOSA, Organización Panamericana de la Salud, Organización Mundial de la Salud, 2021. Informe de situación de los programas de erradicación de la fiebre aftosa en sudamérica y panamá, año 2020. URL: https://www.paho.org/sites/default/files/informe_situacionpaíses-2020-borrador_1.pdf. institutional report, accessed 2024-09-16.
- Pebesma, E., 2018. {Simple Features for R: Standardized Support for Spatial Vector Data}. {The R Journal} 10, 439–446. URL: <https://doi.org/10.32614/RJ-2018-009>, doi:10.32614/RJ-2018-009. publisher: CRAN.
- Perez, A.M., Ward, M.P., Carpenter, T.E., 2004. Control of a foot-and-mouth disease epidemic in Argentina. Preventive Veterinary Medicine 65, 217–226. URL: <https://linkinghub.elsevier.com/retrieve/pii/S0167587704001527>, doi:10.1016/j.prevetmed.2004.08.002.
- Pesciaroli, M., Bellato, A., Scaburri, A., Santi, A., Mannelli, A., Bellini, S., 2025. Modelling the spread of foot and mouth disease in different livestock settings in italy to assess the cost effectiveness of potential control strategies. Animals 15, 386. URL: <https://www.mdpi.com/2076-2615/15/3/386>, doi:10.3390/ani15030386.
- Porphyre, T., Auty, H.K., Tildesley, M.J., Gunn, G.J., Woolhouse, M.E.J., 2013. Vaccination against foot-and-mouth disease: Do initial conditions affect its benefit? PLoS ONE 8, e77616. URL: <https://dx.plos.org/10.1371/journal.pone.0077616>, doi:10.1371/journal.pone.0077616.
- Roche, S.E., Garner, M.G., Sanson, R.L., Cook, C., Birch, C., Backer, J.A., Dube, C., Patyk, K.A., Stevenson, M.A., Yu, Z.D., Rawdon, T.G., Gauntlett, F., 2015. Evaluating vaccination strategies to control foot-and-mouth disease: a model comparison study. Epidemiology and Infection 143, 1256–1275. URL: https://www.cambridge.org/core/product/identifier/S0950268814001927/type/journal_article, doi:10.1017/S0950268814001927.
- Salvarani, F.M., Lins, A.D.M.C., Dos Santos, J.B., Martins, F.M.S., 2025. What to expect from brazil as a nation certified as free from foot-and-mouth disease (FMD) without vaccination. Agriculture 15, 382. URL: <https://www.mdpi.com/2077-0472/15/4/382>, doi:10.3390/agriculture15040382.
- Sanson, R., Rawdon, T., Owen, K., Hickey, K., van Andel, M., Yu, Z., 2017. Evaluating the benefits of vaccination when used in combination with stamping-out measures against hypothetical introductions of foot-and-mouth disease into new zealand: a simulation study. New Zealand Veterinary Journal 65, 124–133. URL: <https://www.tandfonline.com/doi/full/10.1080/00480169.2016.1263165>, doi:10.1080/00480169.2016.1263165.
- Sutmoller, P., Barteling, S.S., Olascoaga, R.C., Sumption, K.J., 2003. Control and eradication of foot-and-mouth disease. Virus Research 91, 101–144. URL: <https://linkinghub.elsevier.com/retrieve/pii/S0168170202002629>, doi:10.1016/S0168-1702(02)00262-9.

- Ulziibat, G., Raizman, E., Lkhagvasuren, A., Bartels, C.J.M., Oyun-Erdene, O., Khishgee, B., Browning, C., King, D.P., Ludi, A.B., Lyons, N.A., 2023. Comparison of vaccination schedules for foot-and-mouth disease among cattle and sheep in mongolia. *Frontiers in Veterinary Science* 10, 990043. URL: <https://www.frontiersin.org/articles/10.3389/fvets.2023.990043/full>, doi:10.3389/fvets.2023.990043.
- Virtanen, P., Gommers, R., Oliphant, T.E., Haberland, M., Reddy, T., Cournapeau, D., Biondi, E., Cross, F., Clifford, P., et al., 2020. SciPy 1.0: fundamental algorithms for scientific computing in Python. *Nature Methods* 17, 261–272. doi:10.1038/s41592-019-0686-2.
- Wickham, H., Averick, M., Bryan, J., Chang, W., McGowan, L., François, R., Grolemund, G., Hayes, A., Henry, L., Hester, J., Kuhn, M., Pedersen, T., Miller, E., Bache, S., Müller, K., Ooms, J., Robinson, D., Seidel, D., Spinu, V., Takahashi, K., Vaughan, D., Wilke, C., Woo, K., Yutani, H., 2019. Welcome to the tidyverse. *Journal of Open Source Software* 4, 1686. URL: <https://joss.theoj.org/papers/10.21105/joss.01686>, doi:10.21105/joss.01686.
- Wittwer, G., 2024. The economic impacts of a hypothetical foot and mouth disease outbreak in australia. *Australian Journal of Agricultural and Resource Economics* 68, 23–43. URL: <https://onlinelibrary.wiley.com/doi/10.1111/1467-8489.12546>, doi:10.1111/1467-8489.12546.
- Wongnak, P., Yano, T., Sekiguchi, S., Chalvet-Monfray, K., Premashthira, S., Thanapongtharm, W., Wiratsudakul, A., 2024. A stochastic modeling study of quarantine strategies against foot-and-mouth disease risks through cattle trades across the Thailand-Myanmar border. *Preventive Veterinary Medicine* 230, 106282. URL: <https://linkinghub.elsevier.com/retrieve/pii/S0167587724001685>, doi:10.1016/j.prevetmed.2024.106282.
- Yadav, S., Delgado, A.H., Hagerman, A.D., Bertram, M.R., Moreno-Torres, K.I., Stenfeldt, C., Holmstrom, L., Arzt, J., 2022. Epidemiologic and economic considerations regarding persistently infected cattle during vaccinate-to-live strategies for control of foot-and-mouth disease in FMD-free regions. *Frontiers in Veterinary Science* 9, 1026592. URL: <https://www.frontiersin.org/articles/10.3389/fvets.2022.1026592/full>, doi:10.3389/fvets.2022.1026592.

A Modelling Assessment of the Impact of Control Measures on Simulated Foot-and-Mouth Disease Spread in Mato Grosso do Sul, Brazil

Supplementary Material and Methods

Model formulation and description

We developed a transmission model that integrates multiple hosts and a single pathogen across different scales to replicate the trajectories of FMD epidemics (Garira, 2018; Cespedes Cardenas and Machado, 2024; Cespedes Cardenas et al., 2024) and enables the simulation of countermeasures. This model resulted in the creation of a software package named **”MHASpread: A multi-host animal spread stochastic multilevel model”** (version 3.0.0). More detailed information at <https://github.com/machado-lab/MHASPREAD-model>. MHASpread enables the explicit definition of species-specific transmission probabilities and the periods during which transmission can occur.

Within-farm dynamics

For the within-farm dynamics, we assumed populations were homogeneously distributed. Species were homogeneously mixed in farms with at least two species, meaning that the probability of contact among species was homogeneous even when species were segregated in barns and/or paddocks (e.g., commercial swine farms are housed in barns with limited chances of direct contact with cattle). The within-farm dynamics comprise mutually exclusive health states (i.e., an individual can be in only one state per discrete time step) for animals of each species (bovines, swine, and small ruminants). Health states (hereafter, “compartments”) include susceptible (S), exposed (E), infectious, (I), and recovered (R), defined as follows:

- **Susceptible:** animals that are not infected and are susceptible to infection.
- **Exposed:** animals that have been exposed but are not yet infectious.
- **Infectious:** infected animals that can successfully transmit infection.
- **Recovered:** animals that have recovered and are no longer susceptible.

Our model accounts for births and deaths, which are used to update the population of each farm. The total population is calculated as $N = S + E + I + R$. The number of individuals within each compartment transitions from $S \xrightarrow{\beta} E$, $E \xrightarrow{1/\sigma} I$, $I \xrightarrow{1/\gamma} R$ according to the following equations:

$$\frac{dS_i(t)}{dt} = u_i(t) - v_i(t) - \frac{S_i(t)I_i(t)}{N_i} \quad (1)$$

$$\frac{dE_i(t)}{dt} = \frac{S_i(t)I_i(t)}{N_i} - v_i(t)E_i(t) - \frac{1}{\sigma}E_i(t) \quad (2)$$

$$\frac{dI_i(t)}{dt} = \frac{1}{\sigma}E_i(t) - \frac{1}{\gamma}I_i(t) - v_i(t)I_i(t) \quad (3)$$

$$\frac{dR_i(t)}{dt} = \frac{1}{\gamma}I_i(t) - v_i(t) \quad (4)$$

Supplementary Table S1: The distribution of each host-to-host transmission coefficient (β) per animal⁻¹ day⁻¹.

Infected species	Susceptible species	Transmission coefficient (β) shape and distribution (min, mode, max)	Reference
Bovine	Bovine	PERT (0.18, 0.24, 0.56)	Calculated from the 2000-2001 FMD outbreaks in the state of Rio Grande do Sul (da Costa et al., 2022)
Bovine	Swine	PERT (0.18, 0.24, 0.56)	Assumed
Bovine	Small ruminants	PERT (0.18, 0.24, 0.56)	Assumed
Swine	Bovine	PERT (3.7, 6.14, 10.06)	Assumed (Eblé et al., 2006)
Swine	Swine	PERT (3.7, 6.14, 10.06)	(Eblé et al., 2006)
Swine	Small ruminants	PERT (3.7, 6.14, 10.06)	Assumed (Eblé et al., 2006)
Small ruminants	Bovine	PERT (0.044, 0.105, 0.253)	Assumed (Orsel et al., 2007)
Small ruminants	Swine	PERT (0.006, 0.024, 0.09)	(Goris et al., 2009)
Small ruminants	Small ruminants	PERT (0.044, 0.105, 0.253)	(Orsel et al., 2007)

Transmission depends on infected and susceptible host species, as reflected by the species-specific FMD transmission coefficient (β) (Supplementary Material Table S1).

The Mato Grosso do Sul database does not consistently record the number of animal births and deaths (excluding those sent to slaughterhouses). Despite this limitation, our model can incorporate these births and deaths whenever data are available. Here, births are represented by the number of animals born alive $u_i(t)$ that enter the S compartment on the farm i at time t according to the day-to-day records; similarly, $v_i(t)$ represents the exit of the animals from any compartment due to death at time t . The transition from E to I is driven by $1/\sigma$, and the transition from I to R is driven by $1/\gamma$; these values are drawn from species-specific distributions derived from the literature (Supplementary Material Table S2).

Supplementary Table S2: The within-farm distribution of latent and infectious periods for FMD in each species.

FMD parameter	Species	Mean, median (25 th , 75 th percentile) in days	Reference
Latent period, σ	Bovine	3.6, 3 (2, 5)	(Mardones et al., 2010)
	Swine	3.1, 2 (2, 4)	(Mardones et al., 2010)
	Small ruminants	4.8, 5 (3, 6)	(Mardones et al., 2010)
Infectious period, γ	Bovine	4.4, 4 (3, 6)	(Mardones et al., 2010)
	Swine	5.7, 5 (5, 6)	(Mardones et al., 2010)
	Small ruminants	3.3, 3 (2, 4)	(Mardones et al., 2010)

Note: The time unit is days.

Kernel transmission dynamics

Spatial transmission encompasses a range of mechanisms, including airborne transmission, animal contact across fence lines, and equipment sharing between farms (Boender et al., 2010; Boender and Hagenaars, 2023). Local spread was modeled using a spatial transmission kernel, in which the likelihood of transmission decreased with distance. The probability P_E at time t describes the likelihood that a farm becomes exposed

and is calculated as follows:

$$P_{E_j}(t) = 1 - \prod_i \left(1 - \frac{I_i(t)}{N_i} \phi e^{-\alpha d_{ij}} \right) \quad (5)$$

where j represents the uninfected population and αd_{ij} represents the distance between farm j and infected farm i , with a maximum of 40 km (Cespedes Cardenas et al., 2024). Given the extensive literature on distance-based FMD dissemination and a previous comprehensive mathematical simulation study (Björnham et al., 2020), distances above 40 km were not considered. Here, $1 - \frac{I_i(t)}{N_i} \phi e^{-\alpha d_{ij}}$ represents the probability of transmission between farms i and j scaled by infection prevalence of farm i , $\frac{I_i}{N_i}$, given the distance between the farms in kilometers. The parameters ϕ and α control the shape of the transmission kernel; $\phi = 0.044$, which is the probability of transmission when $d_{ij} = 0$, and $\alpha = 0.6$ control the steepness with which the probability declines with distance (Boender et al., 2010; Boender and Hagenaars, 2023; Cespedes Cardenas et al., 2024).

FMD spread and control actions

We initially simulated a silent spread over 20 days, generating a broad spectrum of outbreak scenarios before implementing any control measures, as shown in Figure 2. The FMD control scenarios include the following measures: i) depopulation of infected farms, ii) emergency vaccination of farms within the infected and buffer zones, iii) a 30-day standstill on animal movement, and iv) the establishment of three distinct control zones around infected farms: a 3 km infected zone, a 7 km buffer zone, and a 15 km surveillance zone (Supplementary Material Figure S3).

The depopulation of infected farms involves destroying all animals on farms within the infected zone(s), with priority given to farms with larger animal populations. Once depopulated, these farms are excluded from the simulation. When the daily depopulation capacity cannot accommodate all infected farms in a single day, the remaining farms are scheduled for depopulation the following day or as soon as possible, subject to the capacity limits of each simulated scenario (Table 3).

Infected farms detection

Active detection was modeled as a stochastic inspection process applied to farms under surveillance. At each iteration i , detection could only occur among farms that simultaneously met three conditions: (i) they were infected, (ii) they were included in the surveillance zone, and (iii) they had not been detected in previous iterations. This restriction ensures that detection represents newly identified infected farms and avoids double-counting.

Let:

- P_i denote the total number of farms under surveillance at iteration i ,
- I_i denote the number of infected farms within the surveillance population at iteration i ,
- U_i denote the number of infected farms under surveillance that had not yet been detected,
- $k_i = \max(1, \lfloor P_i/3 \rfloor)$ denote the number of farms inspected during iteration i .

The number of farms inspected was defined as one-third of the surveillance population, reflecting limited inspection capacity while ensuring that at least one farm was inspected whenever surveillance was active. If either $P_i = 0$ or $I_i = 0$, no detection was possible, and the detection process was skipped for that iteration.

Detection was modeled as a sampling-without-replacement process. Specifically, the number of infected farms identified during iteration i , denoted by E_i , was drawn from a hypergeometric distribution:

$$E_i \sim \text{Hypergeometric}(M = P_i, n = I_i, N = k_i), \quad (6)$$

where M is the total number of farms under surveillance, n is the number of infected farms within that population, and N is the number of farms inspected. This formulation explicitly accounts for the dependence between inspected farms and the finite size of the surveillance population, which is appropriate for structured livestock systems.

To represent imperfect diagnostic performance, the initially detected farms were further filtered using a binomial process with test sensitivity s :

$$E_i^* \sim \text{Binomial}(E_i, s). \quad (7)$$

This step captures the probability that an infected farm undergoing inspection yields a positive diagnostic result. When $s = 1$, detection is assumed to be perfect, while lower values represent reduced sensitivity due to subclinical infection, sampling error, or diagnostic limitations.

The final number of newly detected farms was constrained such that

$$E_i^* \leq U_i, \quad (8)$$

ensuring that detection could not exceed the number of eligible undetected infected farms. If $E_i^* = 0$, no new farms were added to the detected set. Otherwise, E_i^* farms were randomly sampled from the set of undetected infected farms under surveillance and added to the list of detected farms.

Vaccination

Vaccination was applied exclusively to bovine populations. Bovine farms located within the infected and buffer zones received emergency vaccination 15 days after the establishment of the control zone. Due to logistical capacity constraints, farms that could not be vaccinated within a single day were vaccinated on subsequent days.

The number of farms vaccinated per day varied according to the simulated scenario (Table 2). Vaccination was administered to farms within the infected and/or buffer zones according to predefined prioritization criteria, prioritizing those with the largest animal populations. Once enrolled, each farm was assigned a specific vaccination start day, and animals from the S , E , I , and R compartments were progressively transferred to the V (vaccinated) compartment over successive time steps.

At each time step, the number of animals attempted for vaccination on a given farm was computed as a fixed daily fraction of the total unvaccinated population:

$$a_t = \left\lfloor (S + E + I + R) \cdot \frac{1}{v_t} \right\rfloor \quad (9)$$

where $v_t = 15$ days represents the duration over which the full unvaccinated herd is expected to be processed, and $\lfloor \cdot \rfloor$ denotes the floor function. The attempt a_t was further capped to prevent overshooting the target coverage:

$$a_t = \min(a_t, \max(V^* - V, 0)) \quad (10)$$

where $V^* = \lfloor N \cdot \tau \rfloor$ is the target number of vaccinated animals, N is the total herd size, and τ is the target vaccination coverage (set to 100% in the present study). The number of animals that successfully acquired vaccine-induced immunity was then drawn from a binomial distribution:

$$X \sim \text{Binomial}(a_t, v_e) \quad (11)$$

where v_e denotes the vaccine efficacy, representing the probability that a vaccinated animal develops protective immunity. The X successful animals were subsequently allocated across the S , E , I , and R compartments proportionally to their relative sizes, using a sequential hypergeometric sampling procedure. Specifically, for each compartment k in turn, the number of animals drawn was sampled as:

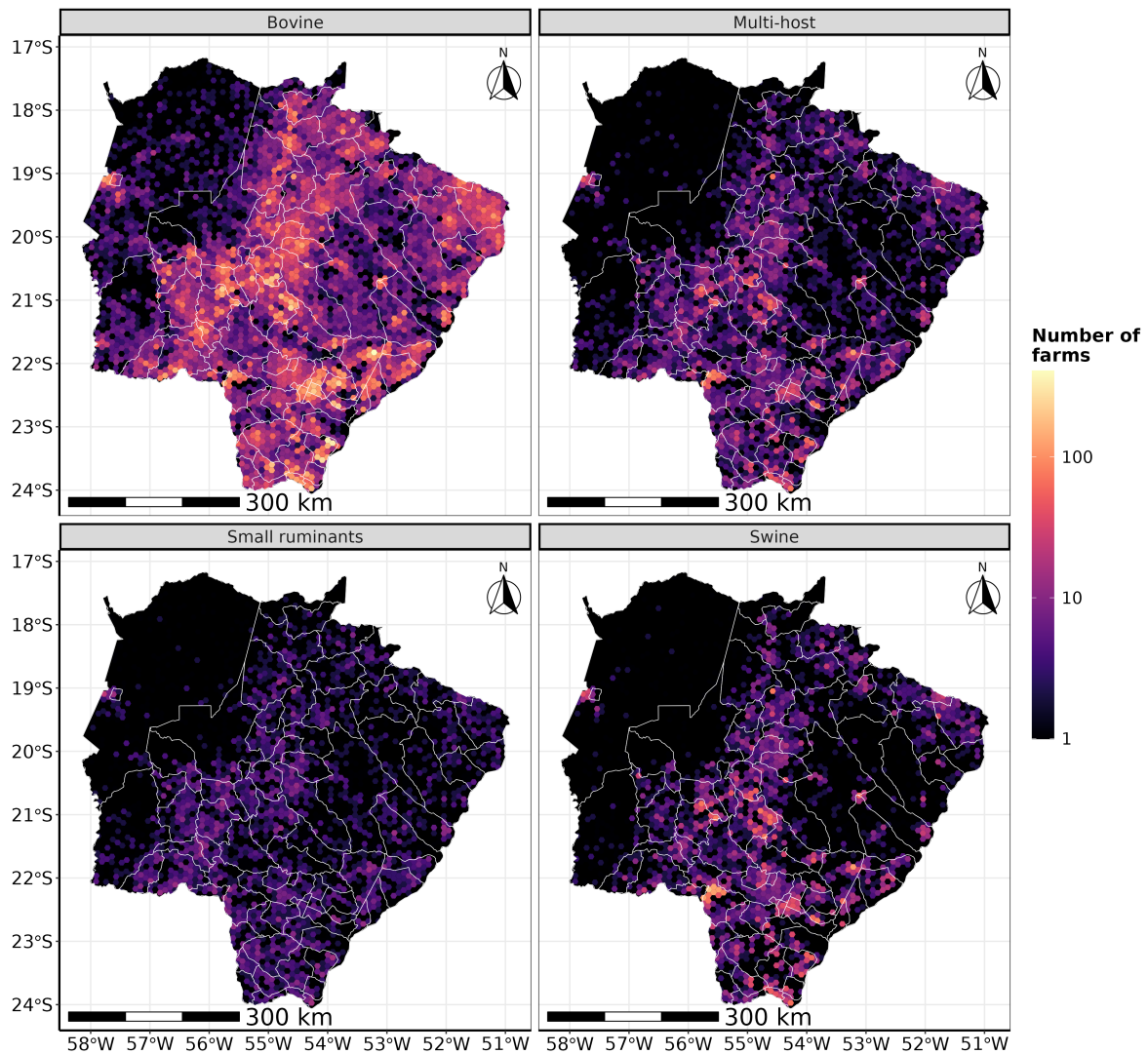
$$d_k \sim \text{Hypergeometric}(C_k, U - C_k, r_k) \quad (12)$$

where C_k is the count of animals in compartment k , U is the total unvaccinated pool at that step, and r_k is the number of successful vaccinations remaining to be allocated. This procedure ensures that animals are removed from each compartment in proportion to its size, without replacement. All allocated animals were transferred to the V compartment. A farm was marked as fully vaccinated and excluded from subsequent processing once the vaccinated population reached the target coverage τ for all enabled species.

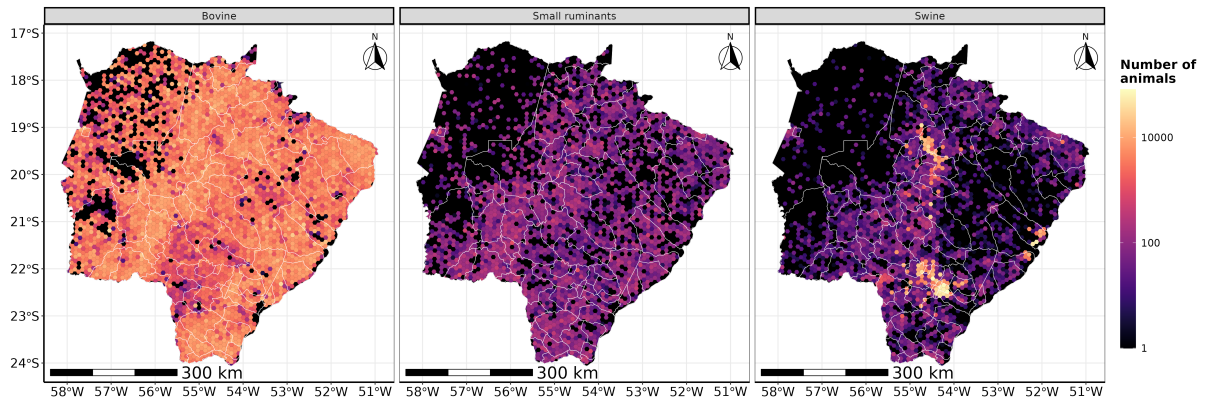
Traceability and movement standstill

We employed contact tracing to identify farms with direct links to infected farms within the past 30 days and subjected these farms to surveillance. Positive farms identified through traceback were categorized as detected infected farms, triggering the application of the same criteria to control zones. In addition, a 30-day restriction on animal movement was enforced across all three control zones, prohibiting both incoming and outgoing movements. The control zones remained in place, and the movement standstill was maintained until depopulation efforts were fully completed.

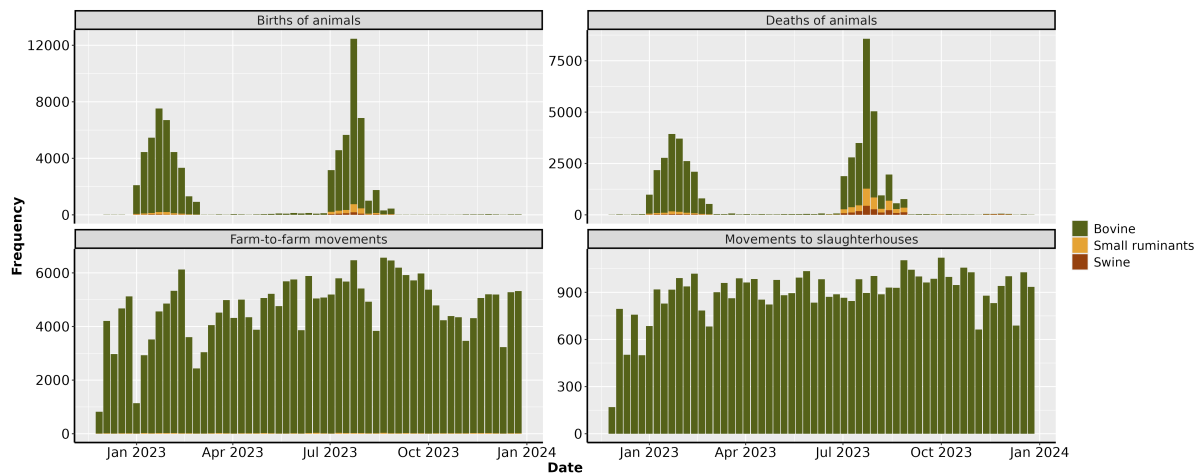
Supplementary Figures



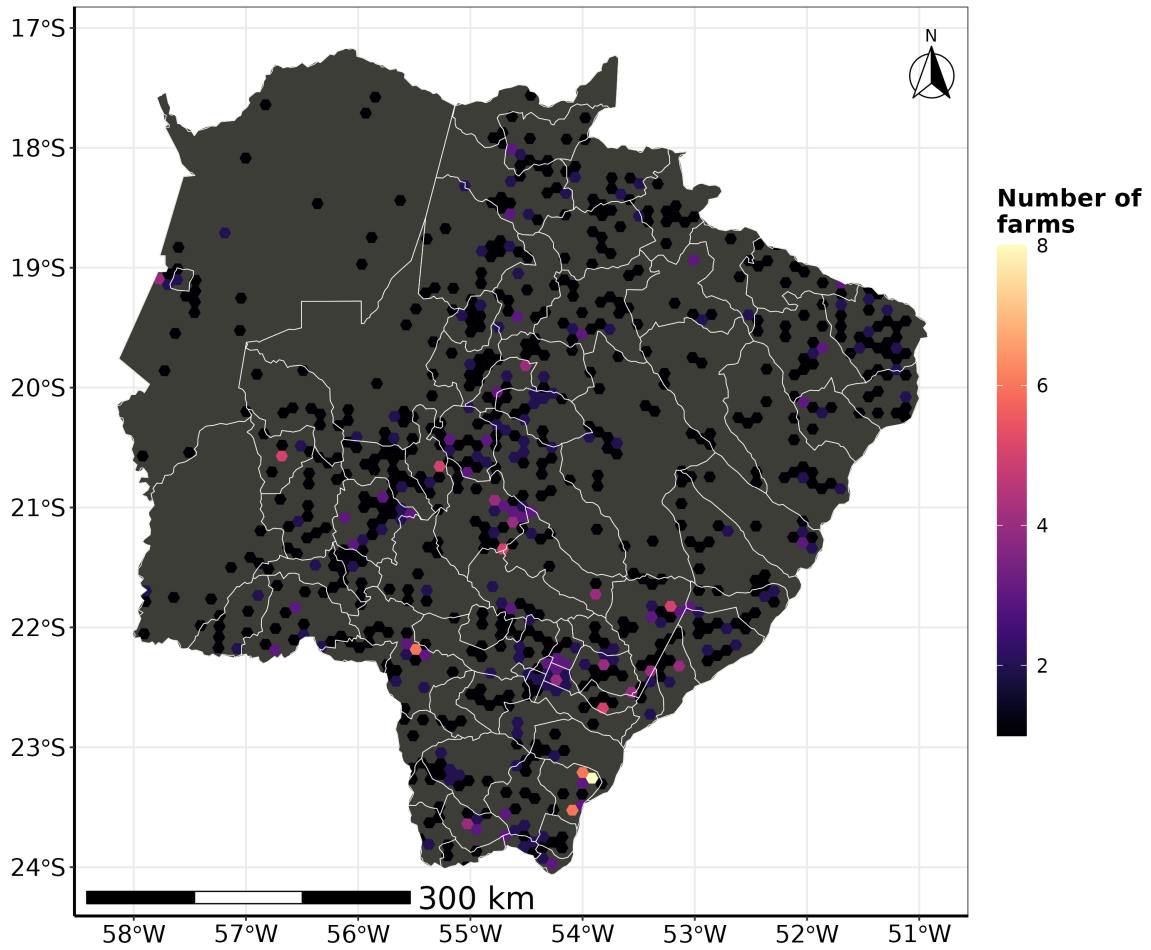
Supplementary Figure S1. Farms density population by species. The size of each hexagon grid is 10 km^2 . The hexagon color represents the number of farms allocated (log10 scale). White lines represent the municipalities' division of Mato Grosso do Sul, Brazil. Each panel shows farms for each species and farms with more than one species.



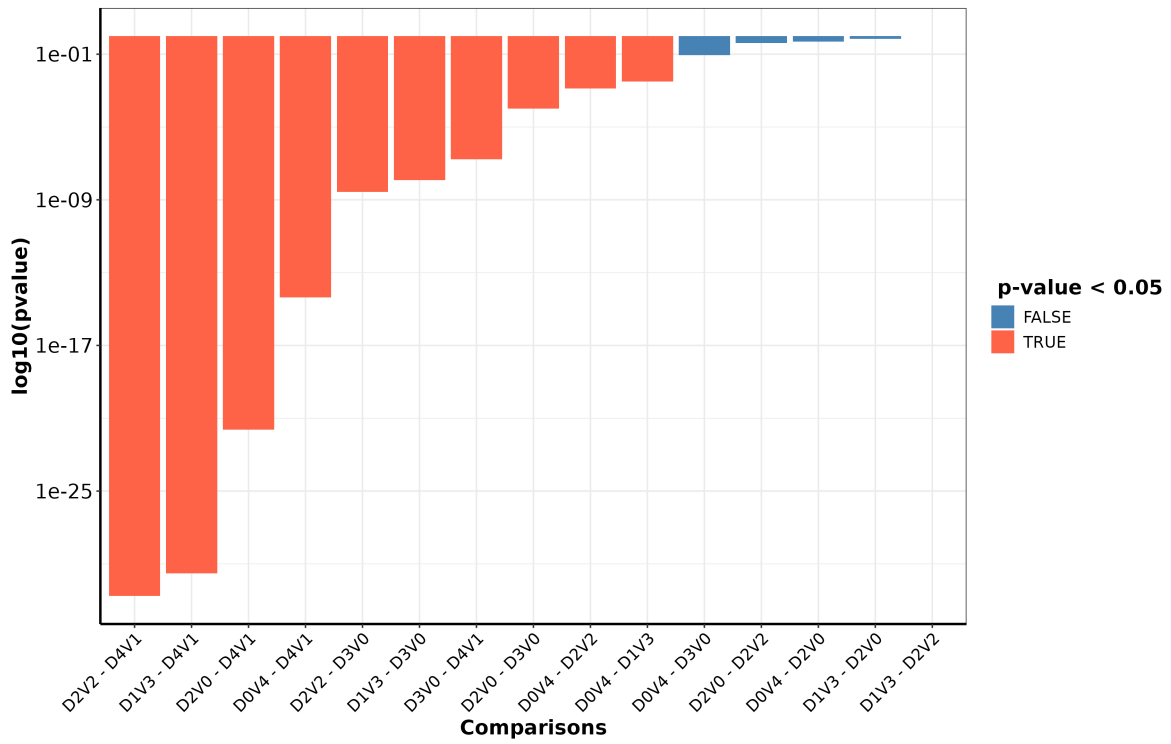
Supplementary Figure S2. Animal density population by species. The size of each hexagon grid is 10 km^2 . The hexagon color indicates the number of animals allocated; note that the color is on a \log_{10} scale. White lines represent the municipalities' division of Mato Grosso do Sul, Brazil. Each panel represents a specific host species.



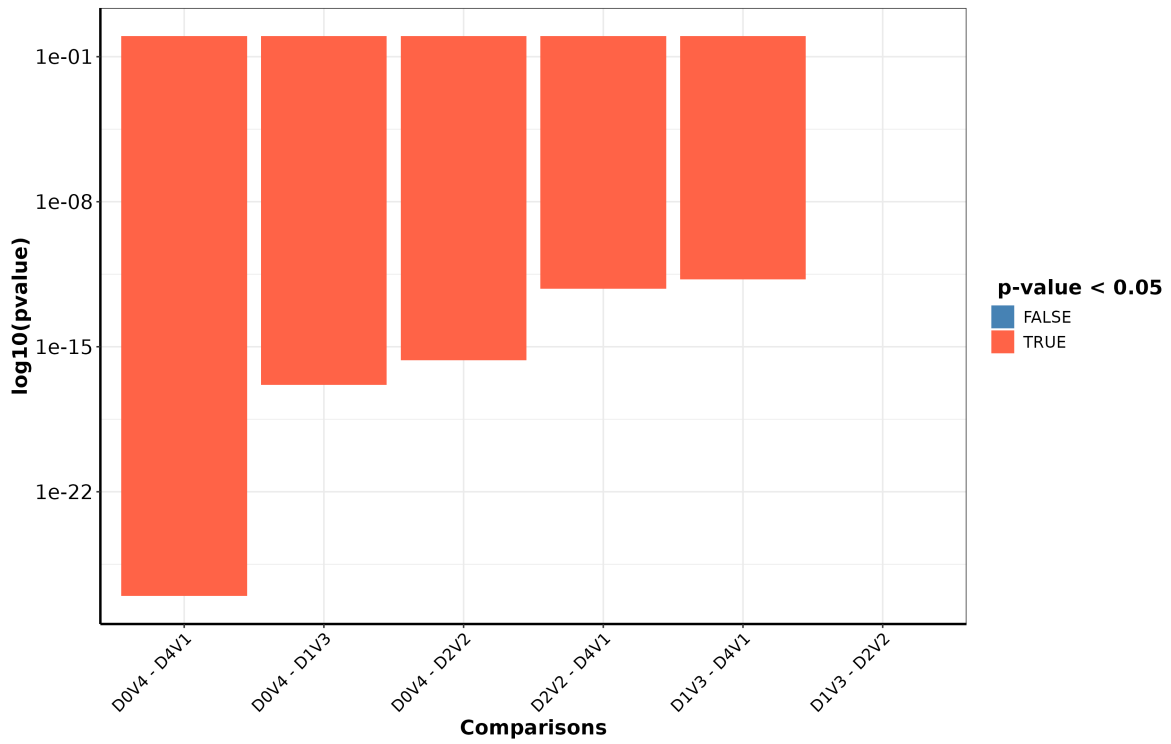
Supplementary Figure S3. Frequency of events by species. The color represents the host species. Each panel represents a specific event.



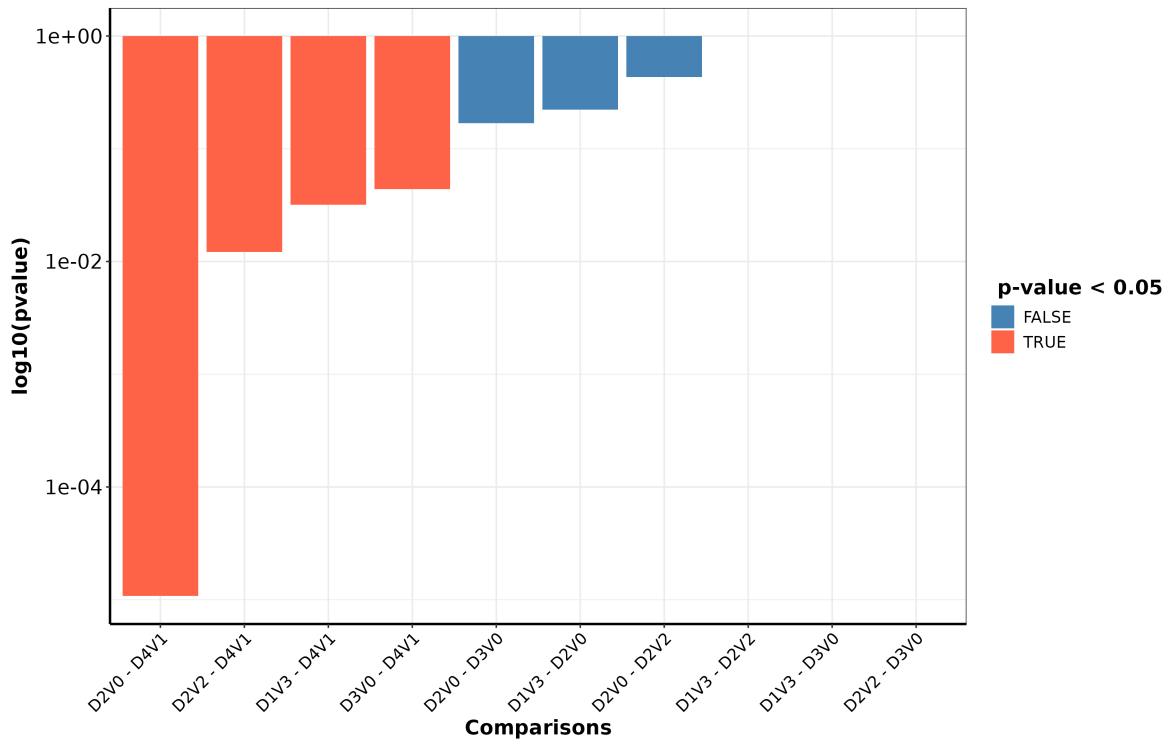
Supplementary Figure S4. The grid density of the sampled farms to seed initial outbreaks. A 10 km² hexagon grid was projected onto the map, and the density was represented as the number of farms allocated in each grid cell. The gray lines represent the political municipal division of Mato Grosso do Sul, Brazil.



Supplementary Figure S5. Results of Dunn’s Test p-values for pairwise comparisons between different scenarios for the total number of infected farms. The y-axis represents the negative log-transformed p-values ($-\log_{10}(\text{p-value})$), with red indicating lower p-values (higher significance) with p-value < 0.05.



Supplementary Figure S6. Results of Dunn's Test p-values for pairwise comparisons between different scenarios for the total number of vaccinated bovines. The y-axis represents the negative log-transformed p-values ($-\log_{10}(\text{p-value})$), with red indicating lower p-values (higher significance) with p-value < 0.05.



Supplementary Figure S7. Results of Dunn’s Test p-values for pairwise comparisons between different scenarios for the total number of depopulated animals. The y-axis represents the negative log-transformed p-values ($-\log_{10}(\text{p-value})$), with red indicating lower p-values (higher significance) with p-value < 0.05.

References

- [1] Björnham, O., R. Sigg, and J. Burman, 2020: Multilevel model for airborne transmission of foot-and-mouth disease applied to Swedish livestock. (Bryan C. Daniels, Ed.) *PLOS ONE* **15**, e0232489, DOI: 10.1371/journal.pone.0232489.
- [2] Boender, G.J., and T.J. Hagenaars, 2023: Common features in spatial livestock disease transmission parameters. *Sci. Rep.* **13**, 3550, DOI: 10.1038/s41598-023-30230-w.
- [3] Boender, G.J., H.J.W. van Roermund, M.C.M. de Jong, and T.J. Hagenaars, 2010: Transmission risks and control of foot-and-mouth disease in The Netherlands: Spatial patterns. *Epidemics* **2**, 36–47, DOI: 10.1016/j.epidem.2010.03.001.
- [4] Cespedes Cardenas, N., F. Amadori Machado, C. Trois, V. Maran, A. Machado, and G. Machado, 2024: Modeling foot-and-mouth disease dissemination in Rio Grande do Sul, Brazil and evaluating the effectiveness of control measures. *Front. Vet. Sci.* **11**.
- [5] Cespedes, N. Cardenas, and G. Machado, 2024: MHASPREAD model. GitHub repository, accessed 16 September 2024. Available at: <https://github.com/machado-lab/MHASPREAD-model>.
- [6] da Costa, J.M.N., L.G. Corbellini, N.C. Cárdenas, F.H.S. Groff, and G. Machado, 2025: Assessing epidemiological parameters and dissemination characteristics of the 2000 and 2001 foot-and-mouth disease outbreaks in Rio Grande do Sul, Brazil. *Ciência Rural* **55**(10), e20240540, DOI: 10.1590/0103-8478cr20240540.
- [7] Eblé, P., A. De Koeijer, A. Bouma, A. Stegeman, and A. Dekker, 2006: Quantification of within- and between-pen transmission of Foot-and-Mouth disease virus in pigs. *Vet. Res.* **37**, 647–654, DOI: 10.1051/vetres:2006026.
- [8] Garira, W., 2018: A primer on multiscale modelling of infectious disease systems. *Infect. Dis. Model.* **3**, 176–191, DOI: 10.1016/j.idm.2018.09.005.
- [9] Goris, N.E., P.L. Eblé, M.C.M. de Jong, and K.D. Clercq, 2009: Quantifying foot-and-mouth disease virus transmission rates using published data. *ALTEX - Altern. Anim. Exp.* **26**, 52–54, DOI: 10.14573/altex.2009.1.52.
- [10] Mardones, F., A. Perez, J. Sanchez, M. Alkhamis, and T. Carpenter, 2010: Parameterization of the duration of infection stages of serotype O foot-and-mouth disease virus: an analytical review and meta-analysis with application to simulation models. *Vet. Res.* **41**, 45, DOI: 10.1051/vetres/2010017.
- [11] Orsel, K., A. Dekker, A. Bouma, J.A. Stegeman, and M.C.M. De Jong, 2007: Quantification of foot and mouth disease virus excretion and transmission within groups of lambs with and without vaccination. *Vaccine* **25**, 2673–2679, DOI: 10.1016/j.vaccine.2006.11.048.